Supplementary Material for the Paper
"Beyond Pairwise Energies: Efficient Optimization for Higher-order MRFs"

Nikos Komodakis
Computer Science Department, University of Crete
komod@csd.uoc.gr

Nikos Paragios
Ecole Centrale de Paris/INRIA Saclay
nikos.paragios@ecp.fr

Abstract

This document contains the proof for theorem 1 of the main paper, as well as experimental results.

1. Proof of theorem 1

Theorem 1. *If there corresponds one sub-hypergraph $G_c = (\mathcal{V}_c, \mathcal{C}_c)$ to each clique c (where $\mathcal{V}_c = \{q | q \in c\}$, $\mathcal{C}_c = \{c\}$), then the algorithm in Fig. 1 of the main paper optimizes the LP relaxation of the following integer LP that is equivalent to problem $\mathrm{MRF}_G(\mathbf{U}, \mathbf{H})$:*

$$\min_{\mathbf{z}} \sum_q \sum_{x_q} U_q(x_q) z_q(x_q) + \sum_c \sum_{\mathbf{x}_c} H_c(\mathbf{x}_c) z_c(\mathbf{x}_c) \tag{15}$$

$$\text{s.t.} \sum\nolimits_{x_q} z_q(x_q) = 1\,, \quad \forall q \tag{16}$$

$$\sum\nolimits_{\mathbf{x}_c : x_q = l} z_c(\mathbf{x}_c) = z_q(l)\,, \quad \forall c \in \mathcal{C}, q \in c \tag{17}$$

$$z_q(\cdot), z_c(\cdot) \in \{0, 1\}\ \ , \tag{18}$$

where a variable $z_q(x_q)$, $z_c(\mathbf{x}_c)$ is associated respectively with each label x_q of node q and each label $\mathbf{x}_c$ of clique c.

Proof. Given any hypergraph $G = \{\mathcal{V}, \mathcal{C}\}$, as well as unary potentials $\mathbf{U} = \mathbf{U}^G = \{\mathbf{U}_q^G\}$ and higher-order potentials $\mathbf{H} = \mathbf{H}^G = \{\mathbf{H}_c^G\}$, the MRF optimization problem $\mathrm{MRF}_G(\mathbf{U}^G, \mathbf{H}^G)$ can be expressed as the following integer LP:

$$\min_{\mathbf{z}^G} E(\mathbf{z}^G, \mathbf{U}^G, \mathbf{H}^G) = \sum_{q \in \mathcal{V}} \mathbf{U}_q^G \cdot \mathbf{z}_q^G + \sum_{c \in \mathcal{C}} \mathbf{H}_c^G \cdot \mathbf{z}_c^G \tag{19}$$

$$\text{s.t.}\ \ \mathbf{z}^{\mathbf{G}} \in \mathcal{Z}^G\ \ , \tag{20}$$

where (for any hypergraph $G = \{\mathcal{V}, \mathcal{C}\}$) the set $\mathcal{Z}^G$ is defined as

$$\mathcal{Z}^G = \left\{ \ \mathbf{z}^G \ \left| \ \begin{array}{ll} \sum_{x_q} z_q^G(x_q) = 1, & \forall\, q \in \mathcal{V} \\ \sum_{\mathbf{x}_c : x_q = l} z_c^G(\mathbf{x}_c) = z_q^G(l), & \forall\, c \in \mathcal{C},\ q \in c \\ z_q^G(\cdot), z_c^G(\cdot) \in \{0, 1\}, & \forall\, q, c \end{array} \right. \right\} \ .$$

In the above problem, the variables are the components of vector $\mathbf{z}^G = \big\{\{\mathbf{z}_q^G\}_{q \in \mathcal{V}}, \{\mathbf{z}_c^G\}_{c \in \mathcal{C}}\big\}$, where we denote $\mathbf{z}_q^G = \{z_q^G(x_q)\}$ and $\mathbf{z}_c^G = \{z_c^G(\mathbf{x}_c)\}$ (*i.e.*, we have introduced one variable $z_q^G(x_q)$ for each label x_q of node q, as well as one variable $z_c^G(\mathbf{x}_c)$ for each label $\mathbf{x}_c$ of clique c).

Given the sub-hypergraph decomposition $\{G_c\}$ described by the theorem, along with the corresponding potentials $\mathbf{U}^{G_c}$ and $\mathbf{H}^{G_c}$ (where $\mathbf{U}_q^{G_c} = \frac{\mathbf{U}_q^G}{|\{c' \in \mathcal{C} | q \in c'\}|}$, $\mathbf{H}^{G_c} = \mathbf{H}_c^G$), the integer LP (19) can be rewritten as follows:

$$\min_{\{\mathbf{z}^{G_c}\}, \mathbf{z}^G} \sum_c E(\mathbf{z}^{G_c}, \mathbf{U}^{G_c}, \mathbf{H}^{G_c}) \tag{21}$$

$$\text{s.t. } \mathbf{z}^{G_c} \in \mathcal{Z}^{G_c}, \ \forall c \in \mathcal{C} \tag{22}$$

$$\mathbf{z}_q^{G_c} = \mathbf{z}_q^G, \ \forall c \in \mathcal{C}, q \in c \ . \tag{23}$$

Here the set of variables $\mathbf{z}^{G_c}$ (one per clique c) denotes:

$$\mathbf{z}^{G_c} = \mathbf{z}_c^G \cup \{\mathbf{z}_q^{G_c}\}_{q \in c} \ , \tag{24}$$

i.e., for defining equivalent problem (21), we have introduced (for each clique c) the extra auxiliary variables $\{\mathbf{z}_q^{G_c}\}_{q \in c}$. Note that the vector of variables $\mathbf{z}^{G_c}$ plays a similar role in slave problem $\mathrm{MRF}_{G_c}(\mathbf{U}^{G_c}, \mathbf{H}^{G_c})$ to that of vector $\mathbf{z}^G$ in master problem $\mathrm{MRF}_G(\mathbf{U}^G, \mathbf{H}^G)$.

The algorithm in Fig. 1 of the main paper is then solving the Lagrangian dual that results from relaxing the constraints (23) in the above integer LP. This Lagrangian dual relaxation is known to be equivalent to the following problem:

$$\min_{\{\mathbf{z}^{G_c}\}, \mathbf{z}^G} \sum_c E(\mathbf{z}^{G_c}, \mathbf{U}^{G_c}, \mathbf{H}^{G_c}) \tag{25}$$

$$\text{s.t. } \mathbf{z}_q^{G_c} = \mathbf{z}_q^G, \ \forall c \in \mathcal{C}, q \in c \tag{26}$$

$$\mathbf{z}^{G_c} \in \mathrm{ConvexHull}(\mathcal{Z}^{G_c}), \ \forall c \in \mathcal{C} \ . \tag{27}$$

Due to (26) and the way $\mathbf{U}^{G_c}$, $\mathbf{H}^{G_c}$ are defined, it holds

$$\sum_c E(\mathbf{z}^{G_c}, \mathbf{U}^{G_c}, \mathbf{H}^{G_c}) = E(\mathbf{z}^G, \mathbf{U}^G, \mathbf{H}^G) \ . \tag{28}$$

Furthermore, due to that G_c containts only one clique, it is easy to show that $\mathrm{ConvexHull}(\mathcal{Z}^{G_c})$ coincides with the set that results from replacing in $\mathcal{Z}^{G_c}$ the integrality constraints with the relaxed constraints $z_q^{G_c}(\cdot) \geq 0, z_c^G(\cdot) \geq 0$. Hence, the above Lagrangian dual (25) coincides with the LP relaxation of the integer program (15), which concludes the proof of the theorem. □

Experimental results

Signal reconstruction

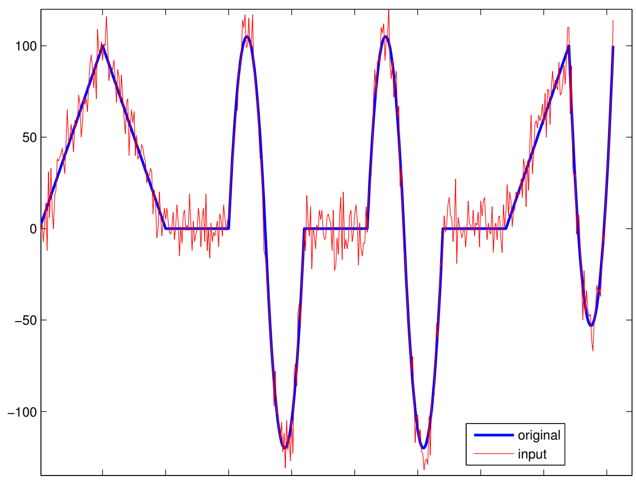

(a) corrupted signal (red) and original signal (blue)

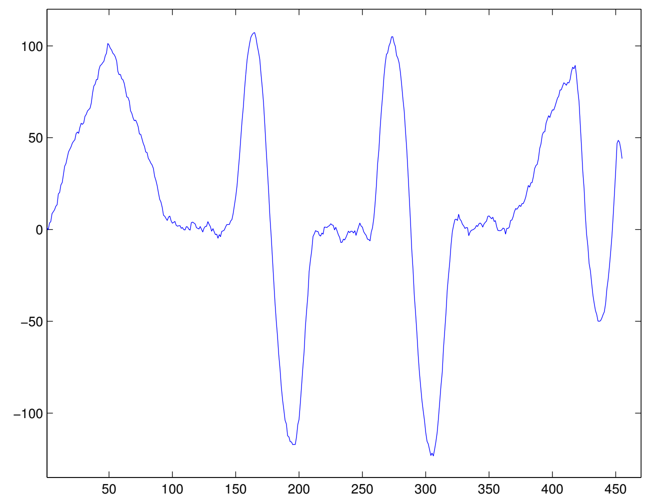

(b) Gaussian filter result

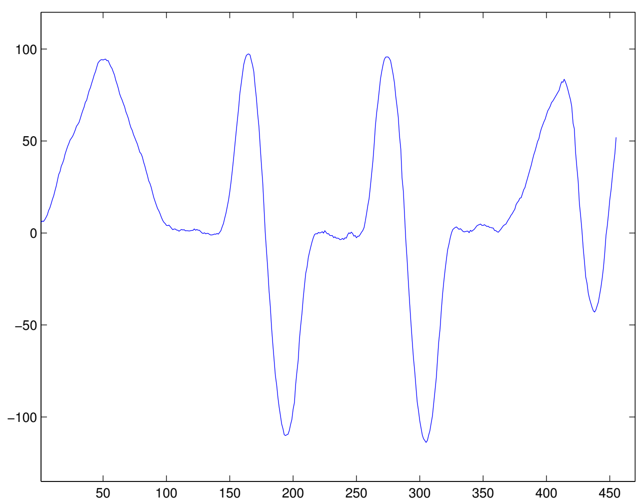

(c) bilateral filter result

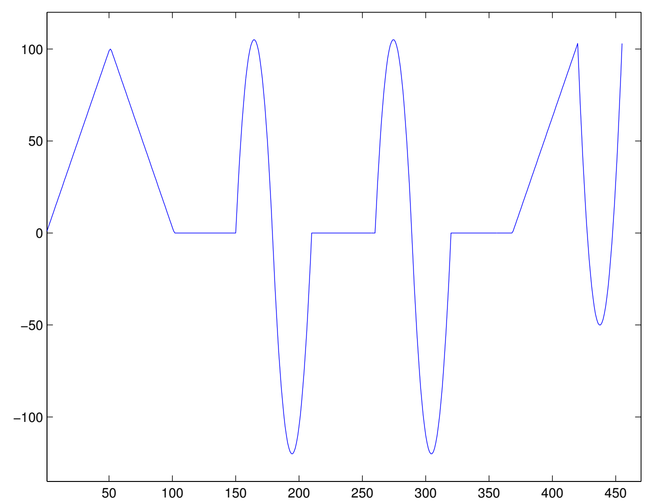

(d) our result with 4^{th}-order MRF

Fig. 11: Signal reconstruction via a 4^{th}-order MRF using potential (12) and 3^{rd}-order derivative filter $\mathcal{F} = [1 \,–3\;\; 3 \,–1]$.

Image denoising

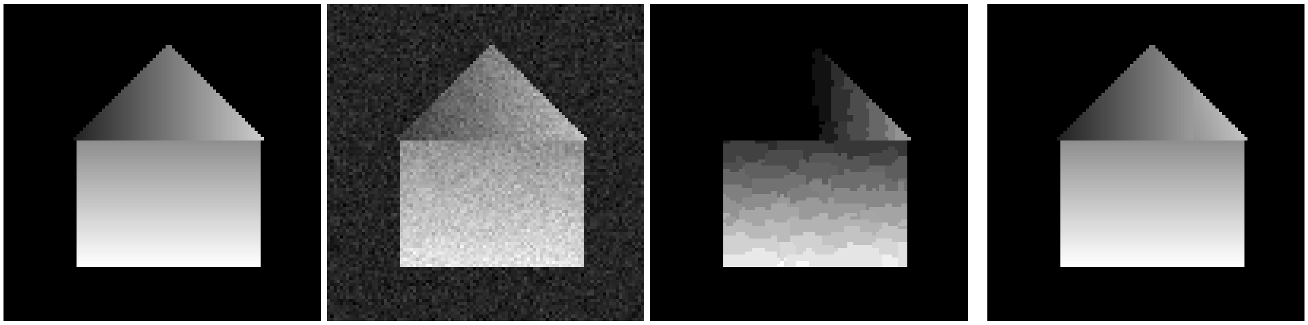

(a) original (b) noisy input (c) pairwise MRF (d) 3^{rd}-order MRF

Fig. 12: Synthetic image denoising via a 3^{rd}-order MRF using potential (12) and filter $\mathcal{F} = [1\ {-2}\ \ 1]$.

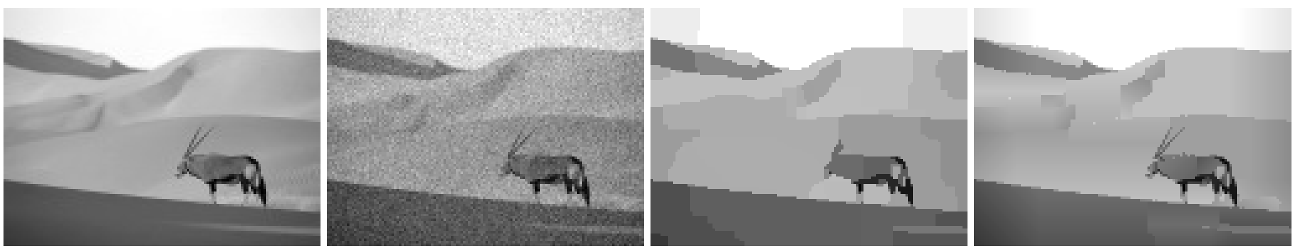

(a) original (b) noisy input (c) pairwise MRF (d) 3^{rd}-order MRF

Fig. 13: Real image denoising via a 3^{rd}-order MRF using potential (12) and filter $\mathcal{F} = [1\ {-2}\ \ 1]$.

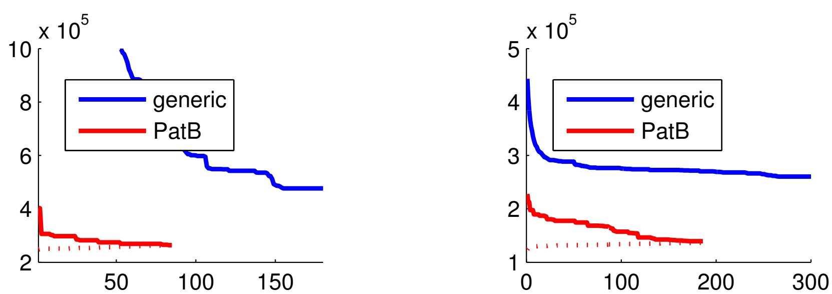

(a) primal-dual costs for the denoising result in Fig. 12

(b) primal-dual costs for the denoising result in Fig. 13

Fig. 14: Primal and dual costs generated by algorithm PatB (drawn in red with solid and dashed lines respectively), as well as primal costs generated by the generic optimizer (drawn in blue).

Stereo matching

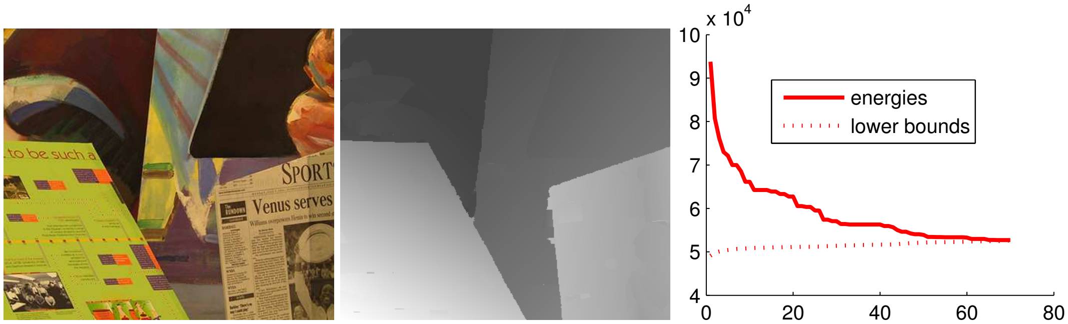

(a) ‘venus’

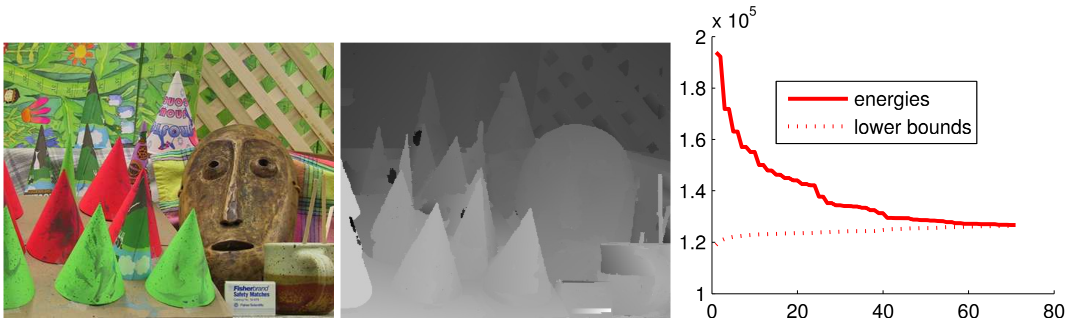

(b) ‘cones’

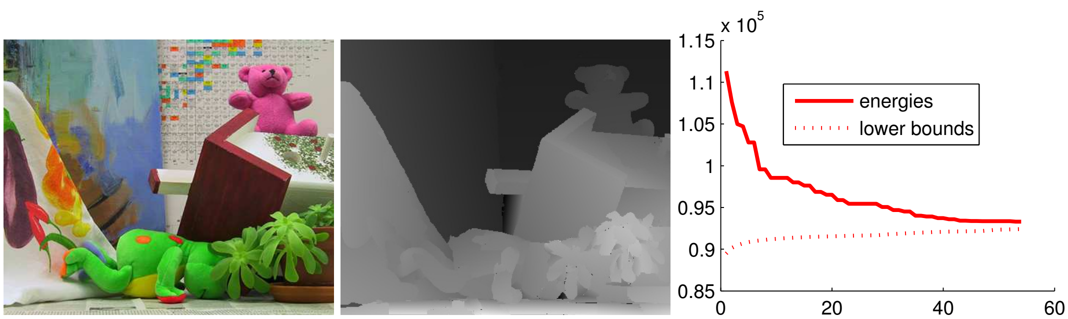

(c) ‘teddy’

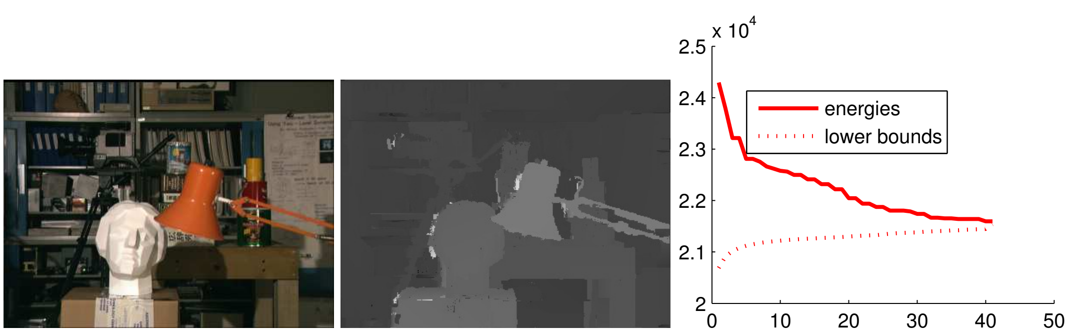

(d) ‘tsukuba’

Fig. 15: Stereo matching results via a 3$^{\mathrm{rd}}$-order MRF using potential (13) and 2$^{\mathrm{nd}}$-order derivative filter $\mathcal{F} = [1\ {-2}\ \ 1]$.

Segmentation, $\mathcal{P}^n$ Potts model

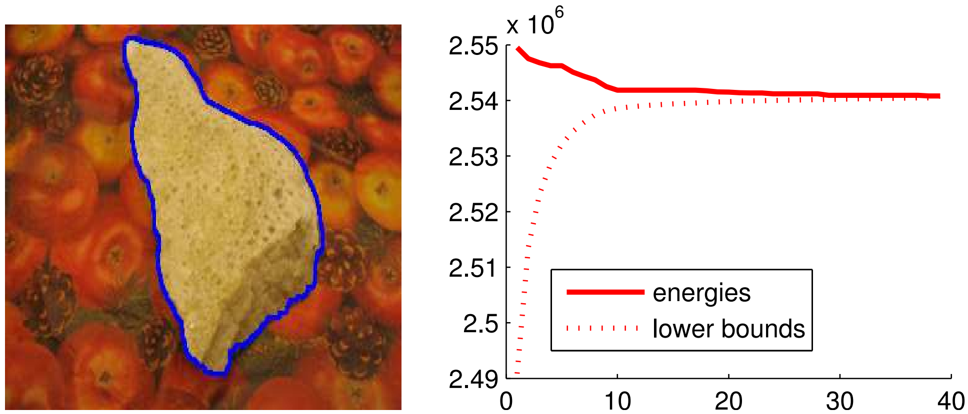

(a) (b)

Fig. 16: Binary image segmentation via $\mathcal{P}^{3\times 3}$ Potts model (global optimum is computed).

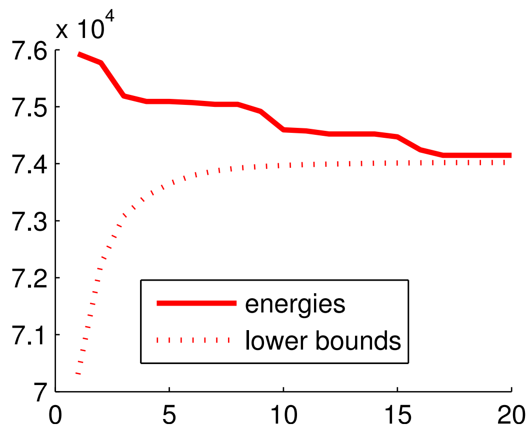

Fig. 17: Optimization for a random $\mathcal{P}^{3\times 3}$ Potts model defined on a 50×50 grid and using 10 labels (global optimum is computed).